Decohesion of iron grain boundaries by sulfur or phosphorous segregation: First-principles calculations

Masatake Yamaguchi,[1] Yutaka Nishiyama,[2] and Hideo Kaburaki[1]
[1]*Center for Computational Science and e-Systems, Japan Atomic Energy Agency, Tokai-mura, Ibaraki-ken 319-1195, Japan*
[2]*Nuclear Safety Research Center, Japan Atomic Energy Agency, Tokai-mura, Ibaraki-ken 319-1195, Japan*
(Received 19 January 2007; revised manuscript received 1 April 2007; published 17 July 2007)

We performed first-principles calculations to simulate the grain boundary decohesion in ferromagnetic bcc iron (Fe) Σ3(111) symmetrical tilt grain boundaries by progressively adding solute atoms [sulfur (S) or phosphorous (P)] to the boundaries. We show that there are two mechanisms of decohesion: (i) fracture surface stabilization with reference to the grain boundary by the segregated solute atoms without interaction between them, and (ii) grain boundary destabilization by a repulsive interaction among the segregated and neighboring solute atoms. It is found that the dominant mechanism for the S-induced decohesion is the former (i), while that for P is the latter (ii). This difference makes P a much weaker embrittling element comparing with S because the mechanism (ii) simultaneously brings about the reduction of the grain boundary segregation energy.

DOI: 10.1103/PhysRevB.76.035418 PACS number(s): 61.72.Mm, 64.75.+g, 68.35.Dv

Although sulfur (S) and phosphorous (P) are famous embrittling elements that segregate to iron (Fe) grain boundaries (GBs) and thereby cause intergranular fracture, it is not well known why and how these elements weaken Fe GBs. The difference in the embrittling ability between S and P is also not well understood. Experiments using Fe-S-C and Fe-P-C alloys indicate that the shift of ductile-to-brittle transition temperature (DBTT) with respect to the S increase in the GB is 40 K, which is two times larger than that by P (20 K).[1] The S-induced GB embrittlement of Fe occurs even when the bulk S concentration is only several tens atomic parts per million (at. ppm, 0.0001 at. %),[2] while the P-induced one occurs when the bulk P concentration is more than ~900 at. ppm.[3]

The change in the cohesive energy (reversible work of fracture) of the GB, 2γ, plays a key role in such intergranular fracture. A ductile-to-brittle transition occurs when the energy release rate of fracture (2γ) becomes smaller than that of the dislocation nucleation and motion at the crack tip.[4] In addition, analyses of the experiments show that the DBTT is inversely related to the total fracture energy Γ, which is the sum of 2γ plus the work of plastic deformation γ_p ($\Gamma = 2\gamma + \gamma_p$).[1,5] Even when γ_p is much larger than 2γ, γ_p should become zero if 2γ is zero; this means that γ_p must depend on 2γ in some way.[6] Therefore, the DBTT correlates inversely with 2γ. Furthermore, 2γ is directly related to the fracture surface energy ($2\gamma_s$) and the GB energy (γ_{gb}), which are affected by segregation through the surface segregation energy ($\Delta E^{seg}_{s,total}$) and the GB one ($\Delta E^{seg}_{gb,total}$),

$$2\gamma = (2\gamma_s - \Delta E^{seg}_{s,total}/A) - (\gamma_{gb} - \Delta E^{seg}_{gb,total}/A). \quad (1)$$

Here, $\Delta E^{seg}_{s,total}$ and $\Delta E^{seg}_{gb,total}$ are defined as the (positive) energy gain for total solute atoms which transfer from the inner bulk region to the surface and the GB, respectively. A is the area of the GB plane on which we consider segregation in a unit cell.

Previously the GB and surface segregation energies for one solute atom ($\Delta E^{seg}_{gb,atom}$, $\Delta E^{seg}_{s,atom}$) were estimated from first-principles calculations.[7] The difference between the two energies, $\Delta E^{seg}_{gb,atom} - \Delta E^{seg}_{s,atom}$, corresponds to the reduction of 2γ. Thus, this energy is called as "embrittling potency energy," which is an important basis for the Rice-Wang thermodynamic theory of intergranular fracture by solute segregation.[1] However, such an energy does not consider an interaction between neighboring solute atoms, and therefore it corresponds to a low concentration case.

Recently, we have shown the importance of the high-segregation-concentration case.[8–10] We found that neighboring S atoms repel each other in fcc Ni Σ5 GB, because the Ni-S bonds are stronger than the S-S bonds. We showed a large reduction of tensile strength (σ_{max}) by one order of magnitude for a high segregation concentration. For a better understanding of this decohesion mechanism from low to high concentration, however, it is necessary to take a look at the reduction of 2γ instead of σ_{max} because 2γ is directly related to the segregation energy as in Eq. (1).

In this paper, we show the reduction of cohesive energy, 2γ, of bcc Fe GB by progressively adding solute (S or P) atoms to the boundary. We clarify quantitatively that the mechanism of S- or P-induced decohesion can be divided into two parts. Schematic illustrations are shown in Fig. 1. The first mechanism (i) is the fracture surface stabilization with reference to the GB by segregated solute atoms without interaction among the atoms. (Here, the interaction means the repulsive one as stated below in the second mechanism.) The basic concept of (i) is the same as the "embrittling potency energy" as stated above. However, we calculate this energy difference quantitatively up to a high concentration range in a realistic situation using bcc Fe Σ3 GB. The second mechanism (ii) is the GB destabilization by a repulsive interaction among segregated and neighboring solute atoms, which has been found in our previous work.[8] This effect occurs after the segregated solute atoms at the GB begin to become neighbors and repel each other; it occurs beyond a critical GB concentration of solute atom (C_1 in Fig. 1). This effect appears as the decrease (or low increase rate) of $\Delta E^{seg}_{gb,total}$ with increasing segregation, which makes solute atoms difficult to segregate.

Interestingly, the main difference in the embrittling effect

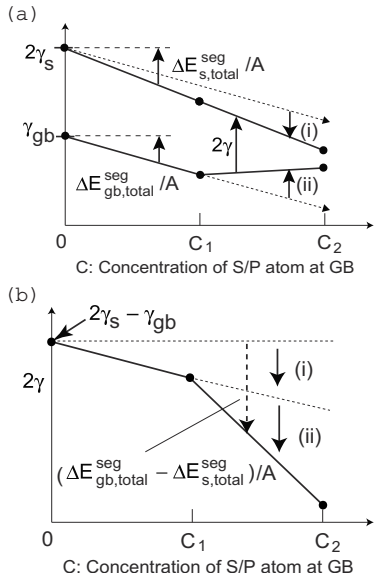

FIG. 1. Schematic illustrations for the decohesion mechanisms. (a) The reduction of surface energy ($2\gamma_s$) and GB energy (γ_{gb}). (b) The reduction of cohesive energy ($2\gamma=2\gamma_s-\gamma_{gb}$). $C \leq C_1$: Segregated solute atoms are apart from each other in the GB. $C_1 < C \leq C_2$: Segregated solute atoms neighbor each other in the GB, but not on fracture surfaces, because the atoms in the GB are divided up between the two fracture surfaces. $C > C_2$: Even on the fracture surface, the solute atoms neighbor and repel each other. The different mechanisms are denoted by (i) and (ii). (b) will be compared with Fig. 7, which shows the calculated results of the cohesive energy 2γ. The calculated 2γ shows a smoother change at the characteristic concentrations of C_1 and C_2 than this schematic figure.

between S and P comes from which one is dominant in the two decohesion mechanisms; the former (i) is dominant for S, while the latter (ii) is dominant for P. Furthermore, the first mechanism is so strong that it overcomes the second mechanism for the S case. The repulsion among segregated S atoms tends to create an incipient fracture surface in the GB, because the surface-stabilization (segregation) energy by S atoms is very large. This surface-stabilization energy compensates for most of the GB destabilization energy by the S-S repulsion. This is the reason why S is easy to segregate in the GB up to a high concentration. For P case, on the other hand, such a compensation does not occur; this makes P atoms difficult to segregate.

We use a bcc Fe $\Sigma 3(111)[1\bar{1}0]$ symmetrical tilt GB in our calculations. Figure 2 shows the unit cell including the GB. Experiments using an iron-1.0 wt. % phosphorous alloy shows that the high-index fracture surfaces have higher segregated P concentrations compared with low-index surfaces, such as the (111) surface.[11] Therefore, we can predict that stronger decohesion occurs at the grain boundaries that consist of higher index planes if the $\Sigma 3(111)$ GB shows a decohesion in our calculations.

Atomic structure relaxation is performed by using the Vienna *ab initio* simulation package (VASP) with projector argumented wave (PAW) potential.[12,13] We use the cutoff energy of 280 eV for the plane-wave basis, the Monkhorst-Pack $3\times4\times1$ k-point mesh, and the Methfessel-Paxton

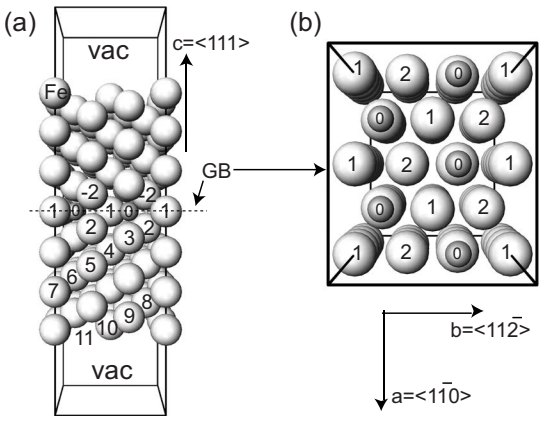

FIG. 2. Unit cell modeling of bcc Fe $\Sigma 3(111)[1\bar{1}0]$ symmetrical tilt GB. A large sphere (radius=0.1 nm) indicates an iron (Fe) atomic site, while a small one (site 0) indicates a GB vacancy site. (a) Side view. Vacuum region (vac) is introduced to allow the GB sliding. (b) Top view of the fracture (111) surface at the GB plane. The area of the GB plane in this cell, A, is 0.556 nm^2 (a =0.801 nm, b=0.694 nm, c=2.55 nm).

smearing with 0.1 eV width. All calculations are done in the ferromagnetic state. The methods of calculation for segregation energy, 2γ, and σ_{max} are summarized in our recent paper.[14] We calculate 2γ as the energy difference between the S- or P-segregated GB and the two fracture surfaces created from the GB, in which the neighboring solute atoms in the GB are divided up between the two surfaces.

First, we show that S and P atoms can segregate to the GB, and that S stabilizes the fracture surface significantly with reference to the GB, while P does not. Figure 3 shows the calculated segregation energy, ΔE^{seg}_{atom}, when one solute atom is substituted for the Fe atom or inserted at various sites in the unit cell (Fig. 2). We can see that the site 0 and 2 are favorable at the GB for both S and P segregation. This is because the nearest-neighbor coordination number is small at these sites; site 0 has two nearest-neighbor Fe atoms (site 3 and -3), and site 2 has only one nearest-neighbor (site -2). On the other hand, the surface-segregation energy at site 10 and 11 for P is much smaller than that for S, although both S and P stabilize the fracture surface more than the GB.

From the calculated segregation energy (ΔE^{seg}_{atom}, as in Fig. 3) we can roughly estimate an equilibrium segregation occupation using McLean's equation,[15] plotted in Fig. 4. This equation indicates that a high bulk solute concentration is necessary for the segregation when the segregation energy is small. Although this equation does not consider the interaction among solute atoms, we think that the occupation can be estimated to a first approximation by replacing ΔE^{seg}_{atom} with the average segregation energy per solute atom ($\Delta E^{seg}_{gb,av} = \Delta E^{seg}_{gb,total}/N_{atom}$, where N_{atom} is the number of solute atoms), even when the interaction occurs.

Second, we show the calculated total ($\Delta E^{seg}_{gb,total}$) and average ($\Delta E^{seg}_{gb,av}$) segregation energy in Fig. 5 when the solute atoms are progressively added to the GB. The $\Delta E^{seg}_{gb,total}$ indicates the total energy gain by segregated solute atoms at the GB. The $\Delta E^{seg}_{gb,av}$ is the energy gain averaged by the num-

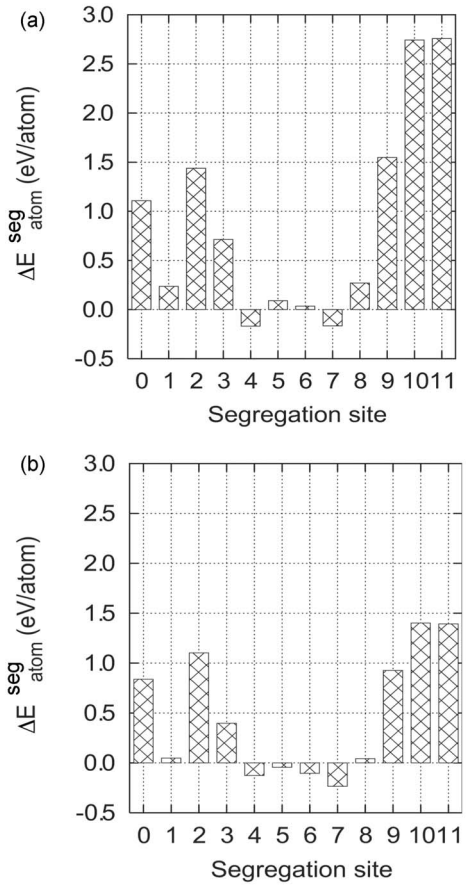

FIG. 3. Calculated segregation energy for one solute atom, ΔE^{seg}_{atom}, at each segregation site (0–11) in the unit cell shown in Fig. 2. Sites 0, 1, 2, 3 are grain-boundary sites, and sites 9, 10, and 11 are surface sites. (a) S, (b) P.

ber of segregated solute atoms (N_{atom}); $\Delta E^{seg}_{gb,av} = \Delta E^{seg}_{gb,total}/N_{atom}$. We determine the atomic configurations of solute segregation as shown in Table I so as to maximize the $\Delta E^{seg}_{gb,total}$ with limited segregation sites (site 0, 2, and -2), which have large segregation energies. The distance between

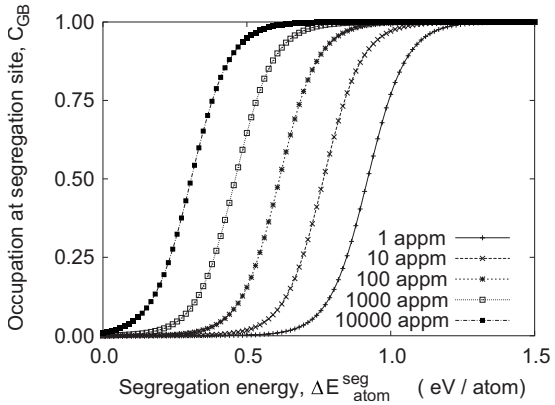

FIG. 4. McLean's equation $\{C_{GB} = C_{bulk}\exp(-\Delta E^{seg}_{atom}/RT)/[1 + C_{bulk}\exp(-\Delta E^{seg}_{atom}/RT)]\}$ is plotted for the aging temperature, T = 773 K, and the bulk concentration of solute atom, C_{bulk} = 1 – 10 000 at. ppm (atomic parts per million).

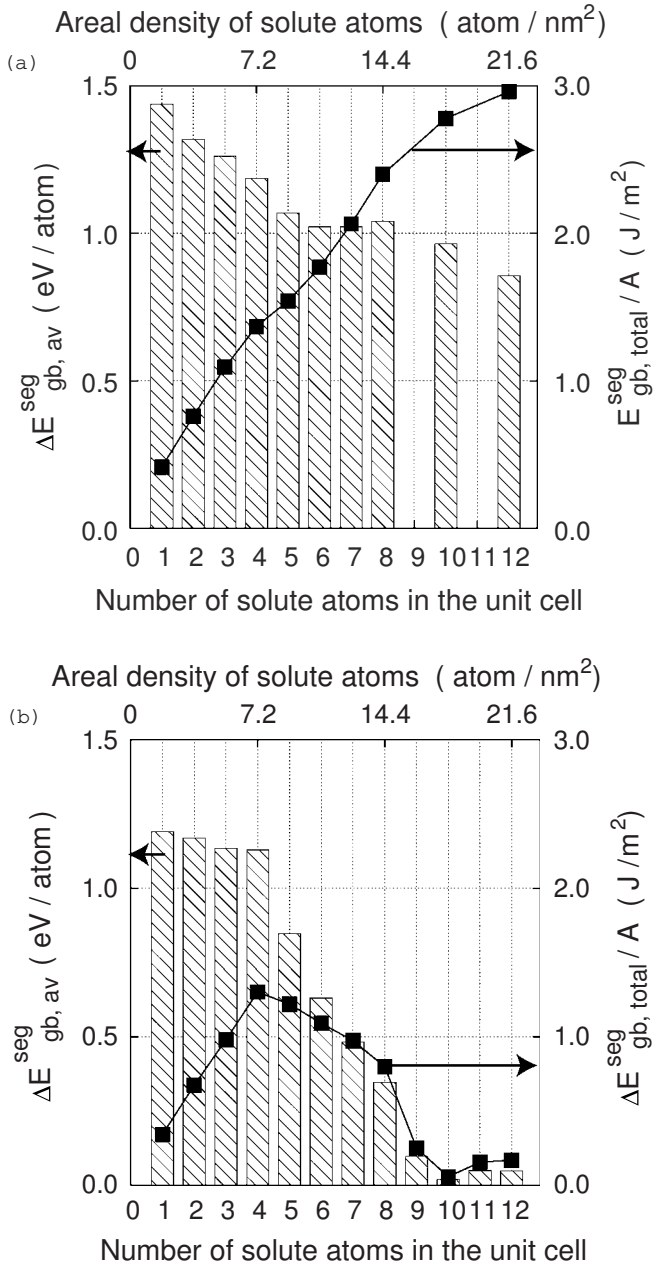

FIG. 5. Calculated total ($\Delta E^{seg}_{gb,total}$, point) and average ($\Delta E^{seg}_{gb,av}$, bar) GB segregation energy for (a) S and (b) P. The $\Delta E^{seg}_{gb,total}$ is divided by the area (A) of the GB plane in the unit cell. The C_1 and C_2 concentrations as explained in Fig. 1 correspond to 4 and 8 solute atoms in this figure, respectively.

the equivalent (same number) sites is large (0.40 nm), and four equivalent sites are included in the unit cell. In this situation, 1–4 solute atoms tend to segregate at the equivalent sites (site 2) because the neighboring solute atoms repel each other. Although the $\Delta E^{seg}_{gb,av}$ decreases from 1 to 4 solute atoms, this is probably not due to the repulsion, but a GB shrinking by a progressive substitution of an undersize solute (S or P) atom for the Fe atom; this shrinking makes the next atom more difficult to segregate. Beyond four atoms in the GB (7.2 atom/nm^2), the repulsion between neighboring solute atoms begins, because they occupy adjacent sites. This

TABLE I. The atomic configurations of segregated solute atoms (S or P) in the GB for each number of segregated solute atoms (N^{seg}_{atom}) that are shown at the horizontal axes in Fig. 5 (segregation energy) and Fig. 7 (cohesive energy). For each number of solute atoms, the occupation of the solute atoms are shown for sites 0, 2, and −2. The distance between the equivalent sites is 0.40 nm. The others are 0.26 nm between sites 0 and 2, and 0.22 nm between sites 2 and −2. (The Fe-Fe distance in bcc Fe is 0.245 nm.)

	S						P					
N^{seg}_{atom}	1	4	5	8	9	12	1	4	5	8	9	12
site 0			1	4	4	4					1	4
site 2	1	4	4	4	4	4	1	4	4	4	4	4
site −2					1	4			1	4	4	4

critical concentration corresponds to a grain boundary concentration, C_1, as in Fig. 1.

From Fig. 5, we can find that S can easily segregate to the GB up to a high concentration, while P cannot. After the S-S repulsion begins (beyond four S atoms), the $\Delta E^{seg}_{gb,av}$ decreases slowly, but the $\Delta E^{seg}_{gb,total}$ still increases. This is because the segregated S atoms can make incipient fracture surfaces in the GB by the S-S repulsion, as in Fig. 6(a), which brings about a large surface stabilization energy, as in Fig. 3, that compensates for most of the energy loss by the S-S repulsion. For the P case, on the other hand, both $\Delta E^{seg}_{gb,total}$ and $\Delta E^{seg}_{gb,av}$ decrease rapidly beyond the four P atoms. In contrast to the S-S repulsion, the P-P repulsion cannot make incipient fracture surfaces at the GB because the surface-stabilization energy by P is much smaller than that by S [Fig. 3(b)]. This can be clearly understood by seeing the electron density maps in Fig. 6. Thus, the energy compensation does not occur for the P-P repulsion.

Third, we show that the S segregation can reduce 2γ by an order of magnitude, while the P segregation is much less effective. Figure 7 shows the calculated 2γ values. By comparing Fig. 7 with Fig. 1(b), we can understand that the dominant mechanism of decohesion with increasing segregation for S is the first mechanism (i), fracture surface stabilization with reference to the GB without interaction among solutes, while that for P is the second mechanism (ii), GB destabilization by a repulsion among neighboring solutes.

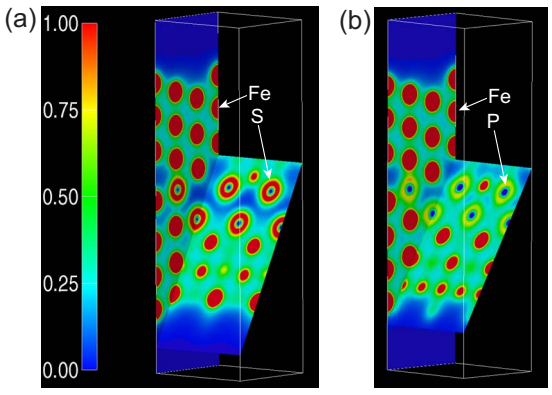

FIG. 6. (Color) Calculated electron density maps (electron/Å^3) for the case of 8 atoms segregated at sites 0 and 2 (two atomic layers, 14.4 atom/nm^2). (a) S, (b) P.

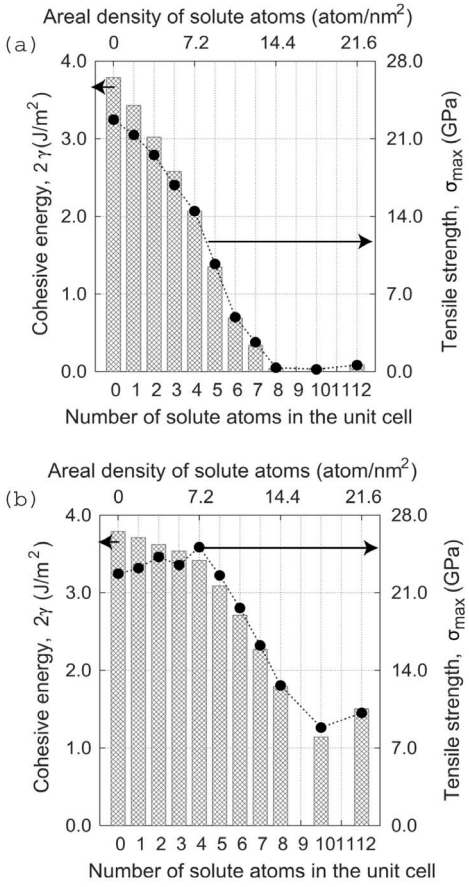

FIG. 7. Calculated cohesive energy (2γ, bar) and tensile strength (σ_{max}, point) with increasing segregation at the GB in the same way as in Fig. 5. (a) S, (b) P.

As shown in Fig. 7(a), the segregated S atoms reduce 2γ rapidly from 1 to 4 S atoms ($C \leq C_1$), and then reduce it a little more rapidly from 4 to 8 S atoms ($C_1 < C \leq C_2$). Finally, 2γ decreases by one order of magnitude at 8 S atoms. The decrease of 2γ for 1 to 4 S segregation is due to the first mechanism (i), because the segregated S atoms do not neighbor each other in the GB (Table I) and they stabilize the fracture surfaces much more than the GB [Fig. 3(a)]. For 4 to 8 S segregation, the decrease of 2γ is accelerated by the S-S repulsion, which destabilizes the GB [the second mechanism (ii)]. However, $\Delta E^{seg}_{gb,av}$ is kept sufficiently high, about 1.0 eV, up to 8 S atoms [Fig. 5(a)]. The energy gain by creating incipient fracture surfaces in the GB compensates for most of the GB destabilization energy by the S-S repulsion, as we explained using Figs. 5 and 6. Therefore, a strong decohesion by one order of magnitude at 8 S atoms (14.4 atom/nm^2) in the GB occurs. This segregation concentration is consistent with fracture surface analyses by Auger electron spectroscopy.[8]

In contrast, the P segregation reduces the 2γ only a little for 1 to 4 P segregation ($C \leq C_1$), as shown in Fig. 7(b). This is because P stabilizes the fracture surfaces only a little with

reference to the GB [Fig. 3(b)]. For 4 to 8 P atoms ($C_1 < C \leq C_2$), the 2γ decreases rapidly. This is due to the destabilization of the GB [the mechanism (ii)] by the neighboring P-P repulsion, which is associated with a significant reduction of $\Delta E_{gb,av}^{seg}$; $\Delta E_{gb,av}^{seg}$ becomes less than 0.5 eV at 8 P atoms [Fig. 5(b)]. This reduction makes P atoms much harder to segregate at the GB than S, as we explained using Fig. 4. These results are consistent with the experimental segregation free energy or enthalpy, 0.3–0.5 (0.8–1.0) eV/atom for P (S),[16] determined in the segregation concentration range in which the embrittlement occurs.

Our calculations indicate that S is a strong embrittling element while P is a weak one, which is consistent with the experiments mentioned in the beginning of this paper. The significant decrease of $\Delta E_{gb,av}^{seg}$ with increasing segregation for the P case [Fig. 5(b)] indicates that the P embrittlement requires a much higher bulk P concentration than the S case. Supposing that $\Delta E_{gb,av}^{seg}$ is 1.0 eV for S and 0.5 eV for P, the required bulk concentration for strong segregation can be estimated from Fig. 4 as about 1 at. ppm for S and 100–1000 at. ppm for P, respectively. This is consistent with the experiments.[2,3] The rate of decrease of 2γ for the S case in the range of 0–4 (4–8) atoms segregation is about 4.0 (1.4) times larger than that for P, as shown in Fig. 7. This is also consistent with the experimental fact that the DBTT shift by S is two times larger than that by P (S: 40 K and P: 20 K for $\Delta 1$ at % in a GB).[1]

We thank Jun Kameda for helpful discussion.

[1] J. R. Rice and J. S. Wang, Mater. Sci. Eng., A **107**, 23 (1989).
[2] S. Suzuki, S. Tanii, K. Abiko, and H. Kimura, Metall. Trans. A **18A**, 1109 (1987).
[3] K. Abiko, S. Suzuki, and H. Kimura, Trans. Jpn. Inst. Met. **23**, 43 (1982).
[4] R. Schweinfest, A. T. Paxton, and M. W. Finnis, Nature (London) **432**, 1008 (2004).
[5] J. Kameda, Acta Metall. **34**, 2391 (1986).
[6] M. L. Jokl, V. Vitek, and C. J. McMahon, Acta Metall. **28**, 1479 (1980).
[7] R. Wu, A. J. Freeman, and G. B. Olson, Science **265**, 376 (1994).
[8] M. Yamaguchi, M. Shiga, and H. Kaburaki, Science **307**, 393 (2005).
[9] W. T. Geng, J. S. Wang, and G. B. Olson, Science **309**, 1677c (2005).
[10] M. Yamaguchi, M. Shiga, and H. Kaburaki, Science **309**, 1677d (2005).
[11] S. Suzuki, K. Abiko, and H. Kimura, Scr. Metall. **15**, 1139 (1981).
[12] G. Kresse and J. Furthmüller, Phys. Rev. B **54**, 11169 (1996).
[13] G. Kresse and D. Joubert, Phys. Rev. B **59**, 1758 (1999).
[14] M. Yamaguchi, M. Shiga, and H. Kaburaki, Mater. Trans., JIM **47**, 2682 (2006).
[15] D. McLean, *Grain Boundaries in Metals* (Oxford University Press, London, 1957).
[16] M. Yamaguchi, M. Shiga, and H. Kaburaki, J. Phys.: Condens. Matter **16**, 3933 (2004).